Inflammation, Vol. 42, No. 1, February 2019 (© 2018)
DOI: 10.1007/s10753-018-0882-8

ORIGINAL ARTICLE

Application of Deacetylated Poly-N-Acetyl Glucosamine Nanoparticles for the Delivery of miR-126 for the Treatment of Cecal Ligation and Puncture-Induced Sepsis

Joy N. Jones Buie,[1] Yue Zhou,[1,2] Andrew J. Goodwin,[3] James A. Cook,[4] John Vournakis,[5] Marina Demcheva,[5] Ann-Marie Broome,[4,6] Suraj Dixit,[6] Perry V. Halushka,[7,8] and Hongkuan Fan[1,9,10]

Abstract— Sepsis is an acute inflammatory syndrome in response to infection. In some cases, excessive inflammation from sepsis results in endothelial dysfunction and subsequent increased vascular permeability leading to organ failure. We previously showed that treatment with endothelial progenitor cells, which highly express microRNA-126 (miR-126), improved survival in mice subjected to cecal ligation and puncture (CLP) sepsis. miRNAs are important regulators of gene expression and cell function, play a major role in endothelial homeostasis, and may represent an emerging therapeutic modality. However, delivery of miRNAs to cells *in vitro* and *in vivo* is challenging due to rapid degradation by ubiquitous RNases. Herein, we developed a nanoparticle delivery system separately combining deacetylated poly-N-acetyl glucosamine (DEAC-pGlcNAc) polymers with miRNA-126-3p and miRNA-126-5p and testing these combinations *in vitro* and *in vivo*. Our results demonstrate that DEAC-pGlcNAc polymers have an appropriate

John Vournakis is deceased. This paper is dedicated to his memory.

[1] Department of Pathology and Laboratory Medicine, Medical University of South Carolina, 173 Ashley Ave., MSC 908, CRI Room 610, Charleston, SC 29425, USA
[2] Department of Biopharmaceutics College of Pharmacy, Nanjing University of Chinese Medicine, Nanjing, 210000, China
[3] Department of Pulmonary, Critical Care, Allergy, and Sleep Medicine, Medical University of South Carolina, Charleston, SC 29425, USA
[4] Department of Neurosciences, Medical University of South Carolina, Charleston, SC 29425, USA
[5] Marine Polymer Technologies, Inc., Burlington, MA 01803, USA
[6] Department of Cell & Molecular Pharmacology and Experimental Therapeutics, Medical University of South Carolina, Charleston, SC 29425, USA
[7] Department of Medicine, Medical University of South Carolina, Charleston, SC 29425, USA
[8] Department of Pharmacology, Medical University of South Carolina, Charleston, SC 29425, USA
[9] Department of Regenerative Medicine and Cell Biology, Medical University of South Carolina, Charleston, SC 29425, USA
[10] To whom correspondence should be addressed at Department of Pathology and Laboratory Medicine, Medical University of South Carolina, 173 Ashley Ave., MSC 908, CRI Room 610, Charleston, SC 29425, USA. E-mail: fanhong@musc.edu

size and zeta potential for cellular uptake and when complexed, DEAC-pGlcNAc protects miRNA from RNase A degradation. Further, DEAC-pGlcNAc efficiently encapsulates miRNAs as evidenced by preventing their migration in an agarose gel. The DEAC-pGlcNAc-miRNA complexes were taken up by multiple cell types and the delivered miRNAs had biological effects on their targets *in vitro* including pERK and DLK-1. In addition, we found that delivery of DEAC-pGlcNAc alone or DEAC-pGlcNAc:miRNA-126-5p nanoparticles to septic animals significantly improved survival, preserved vascular integrity, and modulated cytokine production. These composite studies support the concept that DEAC-pGlcNAc nanoparticles are an effective platform for delivering miRNAs and that they may provide therapeutic benefit in sepsis.

KEY WORDS: Endothelial dysfunction; Polymicrobial sepsis; miRNA delivery; Organ dysfunction; Inflammation.

INTRODUCTION

Sepsis impacts over 1,000,000 people a year and is one of the leading causes of death in intensive care units across the USA [1–3]. It is the most expensive condition to treat in US hospitals, with an economic burden of $20 billion in 2011 and increasing cost of 11.9% annually [1]. Sepsis is characterized by a massive release of inflammatory cytokines that facilitate the activation and trafficking of immune cells. Further, sepsis is frequently complicated by endothelial dysfunction that disrupts the microcirculation and leads to organ failure [4]. Therefore, therapies that blunt cytokine and chemokine release and mitigate endothelial cell damage in sepsis could have enormous therapeutic benefit.

The development of therapies that exploit RNA interference strategies has shown potential for treating cardiovascular, cancer, and inflammatory pathologies. MicroRNAs (miRNAs) are noncoding RNAs that are 21–25 nucleotides in length. MiRNA impacts post-transcriptional regulation of genes by causing gene destabilization and preventing messenger RNA translation [5]. MiRNAs may be effective in preventing endothelial cell damage and improving repair mechanisms in response to cellular stress and inflammation observed in sepsis [6]. MiR-126 is the most abundantly expressed miRNA in endothelial cells and is important for maintaining vascular integrity and angiogenesis [7]. Genetic deletion of pre-miR-126 impedes vascular development, halts angiogenesis, and promotes vascular permeability [8–10], while suppression of miR-126 in the inflammatory microenvironment promotes enhanced expression of VEGF which similarly leads to increased vascular permeability [11].

We recently demonstrated that treatment of murine sepsis with endothelial progenitor cells (EPCs) increases circulating levels of miR-126 while reducing vascular leak and improving survival [12]. Moreover, we observed that EPCs release exosomes with abundant levels of miR-126 [13, 14]. MiR-126 is known to inhibit a variety of genes, which impact endothelial cell homeostasis. Specifically, miR-126-3p targets sprouty-related EVH1 domain-containing protein 1 (Spred1), an inhibitor of angiogenesis, leading to phospho-ERK signaling and cofilin-mediated VE-cadherin stabilization [8]. miR-126-5p targets the NOTCH1 inhibitor DLK-1 enhancing endothelial cell proliferation [15]. Given the potential beneficial effects of miR-126 on endothelial cell function, we postulated that delivery of miR-126 may improve outcomes in sepsis.

Several properties of nucleic acids impair their cellular uptake and potential therapeutic efficacy including their anionic charge, hydrophilicity, and susceptibility to ribonuclease degradation [16]. Thus, the development of a safe and effective miRNA carrier would be of importance for understanding the therapeutic value of miRNAs *in vivo*. We developed a nanoparticle delivery system that is both safe and effective. Deacetylated poly-N-acetyl glucosamine (DEAC-pGlcNAc) has excellent biocompatibility profiles and is biodegradable [17]. DEAC-pGlcNAc is cationic which allows it to form electrostatic interactions with anionic nucleotides like miRNA. Moreover, nanofibers consisting of pGlcNAc have been shown to be antimicrobial [18] while simultaneously supporting wound healing with a favorable safety profile [19]. We tested the ability of DEAC-pGlcNAc to form nanoparticles with miRNAs and thereby serve as a miRNA carrier both *in vitro* and *in vivo* and determine its effects in a model of acute sepsis. We characterized the properties of these nanoparticle complexes, analyzed their ability to protect miRNAs, examined their ability to be taken up by cells and modulate cellular function, and measured their impact on inflammatory cytokine release and survival in a murine model of sepsis. We hypothesized that cationic DEAC-pGlcNAc would form nanoparticles with miRNAs and thereby would successfully deliver active miRNA-126 with minimal toxicity and improve sepsis survival.

MATERIALS AND METHODS

miRNA

Commercially available hsa-miR-126-5p (5'CAUUAUUACUUUUGGUACGCG), hsa-miR-126-3p, (5'UCGUACCGUGAGUAAUAAUGCG), and Allstars negative siRNA-scrambled control were purchased from Qiagen (Valencia, CA). Additionally, Cy3-labeled hsa-miR-126-5p was purchased from GE Healthcare Dharmacon (Lafayette, CO).

Cell Culture

Pooled human umbilical vein endothelial cells (HUVECs) were purchased from Lonza (Walkersville, MD) and cultured in Endothelial Basal Media-2 supplemented with EBM-2 SingleQuots (Walkersville, MD). Cells were cultured at 37 °C in a humidified atmosphere with 5% CO_2. Cell culture media were renewed every 48 h. Cells were passaged at 70% confluence using Trypsin/EDTA (Lonza) and were used at passages 3–5. NIH 3T3 embryonic fibroblast cells were a gift from Dr. Xian Zhang at the Medical University of South Carolina. Cells were cultured in Dulbecco's Modified Eagle's Medium supplemented with 10% fetal bovine calf serum.

Nanoparticle Preparation

Sterile filtered 70% DEAC-pGlcNAc 40 mg/ml (molecular weight ~40,000) and sterile sodium sulfate (50 mM) were obtained from Marine Polymer Technologies (Burlington, MA). Ratio-dependent amounts of miR-126-3p and -5p (0.5–25 μg) were added to 100 μl of a 50 mM sodium sulfate solution at room temperature in order to investigate encapsulation efficiency. Addition of DEAC-pGlcNAc (1.1 mg) was followed by high-speed vortexing for 20 s. Complex self-assembly occurred at room temperature for 15 min. The nanopolymer mixture was neutralized using 0.5 M NaOH with additional vortexing for 10 s. Following neutralization, the final pH of the complexes was 7. For RNase A and encapsulation studies, the formulations were pelleted by centrifugation (15,000 rpm, 4 °C for 1 h, 5424R Centrifuge, Beckman) for further analysis. The N/P ratio was calculated using the following equation:

$$\frac{N}{P} = \frac{\text{number of moles of cationic DEAC-pGlcNAc} \times 150 \text{ amine groups}}{\text{number of moles of miRNA} \times 44 \text{ phosphate groups}}$$

Four different ratios of DEAC-pGlcNAc were generated 50:1, 700:1, 1400:1, and 2700:1 which contained 24.48 μg, 1.8 μg, 0.9 μg, and 0.45 μg of miRNA, respectively.

Nanoparticle Characterization

Following formulation, DEAC-pGlcNAc:miRNA nanoparticles were centrifuged and supernatant was removed. Nanoparticles were then suspended in 20 μl of 50 mM sodium sulfate solution and placed on a stainless steel TEM grid and covered with 2% uranyl acetate for 30 s. Samples were rinsed in ultra-purified water and allowed to dry in a desiccator and imaged using a JEOL 1010 transmission electron microscope (Peabody, MA) with a Hamamatsu C4742-95 digital camera (Hamamatsu City, Japan). We determined size and zeta (*Z*) potential of the DEAC-pGlcNAc nanocomplexes using dynamic light scattering methodology (DLS) (Zetasizer, Nano ZS, Malvern, UK, and ZetaPALS, Brookhaven Instruments Corp).

Electrophoretic Mobility Gel Shift Assay

The binding of DEAC-pGlcNAc and miR-126 was evaluated using a 4% (*w*/*v*) agarose E-gel and iBase system containing ethidium bromide. Briefly, nanocomplexes were formed and 20 μl of sample were added to the gel. The iBase electrophoresis was run based on the manufacturer's recommendations. The miR-126 bands were analyzed using a UVP transilluminator (Alpha Innotech Corporation, Santa Clara, CA).

Evaluation of Encapsulation Efficiency

To evaluate the encapsulation efficiency of miRNA by DEAC-pGlcNAc, a standard curve using naked miRNA was generated. Briefly, various concentrations of miRNA were electrophoresed in a 4% (*w*/*v*) agarose E-gel using the iBase system for 30 min. Simultaneously, 4% SDS-treated nanocomplexes were resolved in the same gels. The gel was analyzed using a gel doc system and bands were analyzed using image J. The standard curve was generated based on band intensity and the concentrations of encapsulated RNA were calculated based on the standard curve.

RNase A Protection Assay

The ability of DEAC-pGlcNAc to protect miRNA from RNase A enzyme was evaluated. Nanocomplexes and control naked miR-126-5p were treated with 0.18 μg RNase A for 1 h at 37 °C. Complexes were pelleted using centrifugation (15,000 rpm, 25 °C) and treated with 4 μl EDTA (0.25 M) for 10 min. Pellets were then re-suspended in 2% SDS and allowed to sit for 30 min prior to gel

electrophoresis. Treated nanocomplexes and naked miRNA underwent gel electrophoresis using a 4% (*w*/*v*) agarose E-gel using the iBase system for 30 min and were then analyzed.

MTT Assay

The viability of HUVECs following treatment with various ratios of DEAC-pGlcNAc:miRNA nanocomplexes was assessed using the MTT (3-(4,5-dimethylthiazole-2-yl)-2,5-diphenyl tetrazolium bromide) assay. Approximately, 2.0×10^4 cells/well were allowed to adhere overnight in a 96-well plate. Media were replenished and cells were treated with varying N/P molar ratio nanocomplexes. After 24-h incubation, cells were washed and the MTT solution was added. Cells were incubated at 37 °C for 4 h and the formazan was dissolved in acidic isopropanol. The viability of cells was assessed using a Synergy 4 microplate reader (BioTek) at absorbance 570 nm with background subtraction at 630–690 nm.

Fluorescence Microscopy

Complexes were formed using fluorescently labeled DEAC-pGlcNAc and Cy3-labeled-miRNA. HUVECs were treated for 24 h with 25 μl of the total complex, yielding molar concentrations of 55 nM, 27.5 nM, and 14 nM, respectively. Complexes were removed and cells were washed with PBS and fixed using 4% paraformaldehyde (PFA) for 20 min. Upon PFA removal, slides were mounted with a glass coverslip using ProLong® Gold antifade reagent with DAPI (Thermo Fisher Scientific, Eugene, OR). Fluorescent images were acquired using an Olympus IX73 research inverted microscope (Olympus) equipped with a LUCPlan FLN 40X/0.60 Ph2 objective.

In Vitro Cellular Uptake and Quantitative Real-Time RT-PCR of miRNAs

HUVECs and NIH 3T3 fibroblasts were seeded at a density of 1.0×10^5 cells per well. Cells were allowed to adhere overnight and then treated with 25 μl of nanocomplexes for 24 h. miRNA was isolated using MiRNeasy Kit (Qiagen). RNA integrity was assessed using a BioTek Gen5™ (Winooski, Vermont) plate reader Take 3 software. For each reaction, 1 μg of miRNA was used for cDNA synthesis using a miScript II RT Kit (Qiagen). cDNA product was amplified with miScript SYBR Green PCR Kit. A CFX96 real-time PCR detection system (Bio-Rad, Hercules, CA) was used to assess changes in hsa-miR-126-3p and -5p, and RNU6B as internal control.

Fibroblast Growth Factor-Mediated ERK Phosphorylation

HUVECs seeded in 6-well plates were incubated with nanocomplexes at 50:1 containing 1.0 μg per well of negative siRNA (Allstars, Qiagen) or miR-126-3p for 24 h. HUVECs were completely serum-starved with EBM-2 basal medium for 16 h and then treated with fibroblast growth factor (FGF-2, 10 ng/ml) for 15 or 45 min. HUVECs were then placed on ice, washed in ice-cold PBS, and lysed with RIPA Buffer (50 mM Tris-HCl pH 8.0, 150 mM NaCl, 1% Nonidet P-40 (NP-40), 0.5% sodium deoxycholate, 0.1% sodium dodecyl sulfate (SDS), 1 mM sodium orthovanadate, 1 mM NaF) supplemented with a protease/phosphatase inhibitor and okadaic acid (20 nM; Cell Signaling). Protein lysates were resolved in a 4–12% Bis-Tris Protein Gel at 100–200 V for 1.5 h. Proteins were transferred to a PVDF membrane at 100 V for 1 h and blocked using Odyssey Blocking Buffer (Li-Cor) for 1 h. Blots were probed with phospho-ERK 42/44 (1:1000), total ERK 42/44 (1:1000) overnight at 4 °C. Blots were analyzed using an Odyssey Licor Imaging System (Li-COR).

DLK-1 Western Blots

For DLK-1 experiments, HUVECs seeded in 6-well plates were incubated with nanocomplexes at a 50:1 ratio containing 1.0 μg of negative siRNA (Allstars, Qiagen) or miR-126-5p for 48 h. The cellular proteins were extracted and lysates were processed as described above. Blots were probed for α-tubulin (1:1000; Cell Signaling), or DLK-1 (1:1000; Abcam) overnight at 4 °C and IRDye secondary antibodies (1:10000) for 1 h. Blots were analyzed using an Odyssey Licor Imaging System (Li-COR).

Cecal Ligation and Puncture (CLP)

CLP was performed in CD-1 male mice, aged 7–8 weeks old as previously described [20]. Briefly, after ligation with a 5–0 suture, a 22-gage needle was used to produce two punctures in the cecum, after which the surgical site was closed with clips. All mice received saline subcutaneously after closure of the abdominal opening. Investigations were conducted in accordance with the Guide for the Care and Use of Laboratory Animals published by the National Institutes of Health and were approved by the Institutional Animal Care and Use

Committee at the Medical University of South Carolina. Mice were subjected to CLP and administered PBS, DEAC-pGlcNAc (5 mg/kg), or DEAC-pGlcNAc:miR-126-3p or DEAC-pGlcNAc:miR-126-5p nanocomplexes (700:1 complex; 0.4 μg per mouse/ per injection) *via* tail vein injection 2 h and 6 h after CLP. The antibiotic imipenem (25 mg/kg, subcutaneously) was administered at 6 h, 24 h, and 48 h after CLP.

Blood Collection and Serum Isolation and Analysis

CD-1 mice previously subjected to CLP surgery were euthanized using isoflurane and blood was collected from the inferior vena cava 24-h post-CLP surgery. Blood samples were kept at 25 °C for 30 min. Samples were centrifuged at 10,000 g for 10 min at 25 °C. The serum fraction was collected and stored at − 80 °C prior to blood chemistry analysis. Blood chemistries were analyzed in the mouse pathology facility at MUSC. Mouse serum samples were shipped on dry ice to Eve Technologies (Calgary, Alberta, Canada) where a mouse cytokine-32 plex discovery assay was conducted.

Vascular Permeability Assay

CD-1 mice were subjected to CLP and administered PBS, DEAC-pGlcNAc, or DEAC-pGlcNAc:miR-126-3p or DEAC-pGlcNAc:miR-126-5p nanocomplexes *via* tail vein injection 2 h and 6 h after CLP as described above. Vascular permeability was quantified 24-h post-CLP using an Evans blue dye as previously described [12]. Briefly, 1% Evans blue (Sigma) dye was dissolved in saline solution. Two hundred microliters of Evans blue dye was slowly injected into the tail vein of the mice using a syringe void of air bubbles. After 40 min, the mice were sacrificed and perfused *via* the heart with PBS, and the lung and kidney tissues were collected. The lung and kidney weights were measured and placed in 1 ml of formamide (Avantor) at 60 °C for 24 h to extract Evans blue. Following centrifugation at 2000 rpm for 10 min, the supernatant was collected. Evans blue in the lung and kidney tissues was quantified using spectrophotometric analysis at 620 nm. Evans blue concentrations were extrapolated from a standard curve. The permeability index was calculated based on the extrapolated concentrations and normalized to the tissue weight.

Statistical Analysis

Data are expressed as mean ± standard error of the mean (SEM). RT-PCR data were analyzed using ANOVA with Tukey's post-test or the Kruskal-Wallis test if data was not normally distributed. pERK western blot data was analyzed using a two-way ANOVA, matching both factors. Student's *t* test was used to analyze DLK-1 data. Survival analysis was performed using the Gehan-Breslow-Wilcoxon test. The Evans blue data was analyzed using a one-way ANOVA. Cytokine expression data were analyzed using the Kruskal-Wallis or ANOVA tests as appropriate. All statistical analysis was performed using GraphPad Prism 7 software. A p value of < 0.05 was used to reject the null hypothesis.

RESULTS

DEAC-pGlcNAc Polymer Effectively Binds and Protects miRNA from RNase A Degradation

We chose to use DEAC-pGlcNAc nanoparticles as a delivery system for the miRNAs because they have non-specific antibacterial properties [18] and we hypothesized that miR-126 might provide additive or synergistic effects for the treatment of sepsis. DEAC-pGlcNAc nanoparticles were prepared as described in the methods. We performed an electrophoretic mobility shift assay using agarose gel to determine how effectively DEAC-pGlcNAc bound miRNA. The assay demonstrated that across all concentrations, miRNA was thoroughly bound to DEAC-pGlcNAc and unable to migrate through the gel matrix (Fig. 1a). The nanocomplexes and control naked miRNA were also incubated with RNase A for 60 min. Minimal miRNA degradation was observed in the 50:1, 700:1, and 1400:1 complexes incubated with RNase A while substantial degradation did occur in the 2700:1 complex (Fig. 1b, c). Densitometry analysis suggested that DEAC-pGlcNAc at 700 and 1400 M excess protected 90% of the miRNA from degradation (Fig. 1c, densitometry analysis not shown). Additionally, we sought to determine the optimal encapsulation efficiency of 700:1, 1400:1, and 2700:1 nanocomplexes. At a ratio of 700:1, approximately 80% of the miRNA was encapsulated while at ratios of 1400:1 and 2700:1, only about 50% of the miRNA was encapsulated (Fig. 1d, e).

Optimization of the DEAC-pGlcNAc:miR-126 Complex

In order to confirm that the nanocomplexes facilitate the cellular uptake of miRNAs, we incubated fluorescently labeled DEAC-pGlcNAc:cy3-miRNA-126-5p complexes with HUVECs for 24 h and then analyzed the subcellular

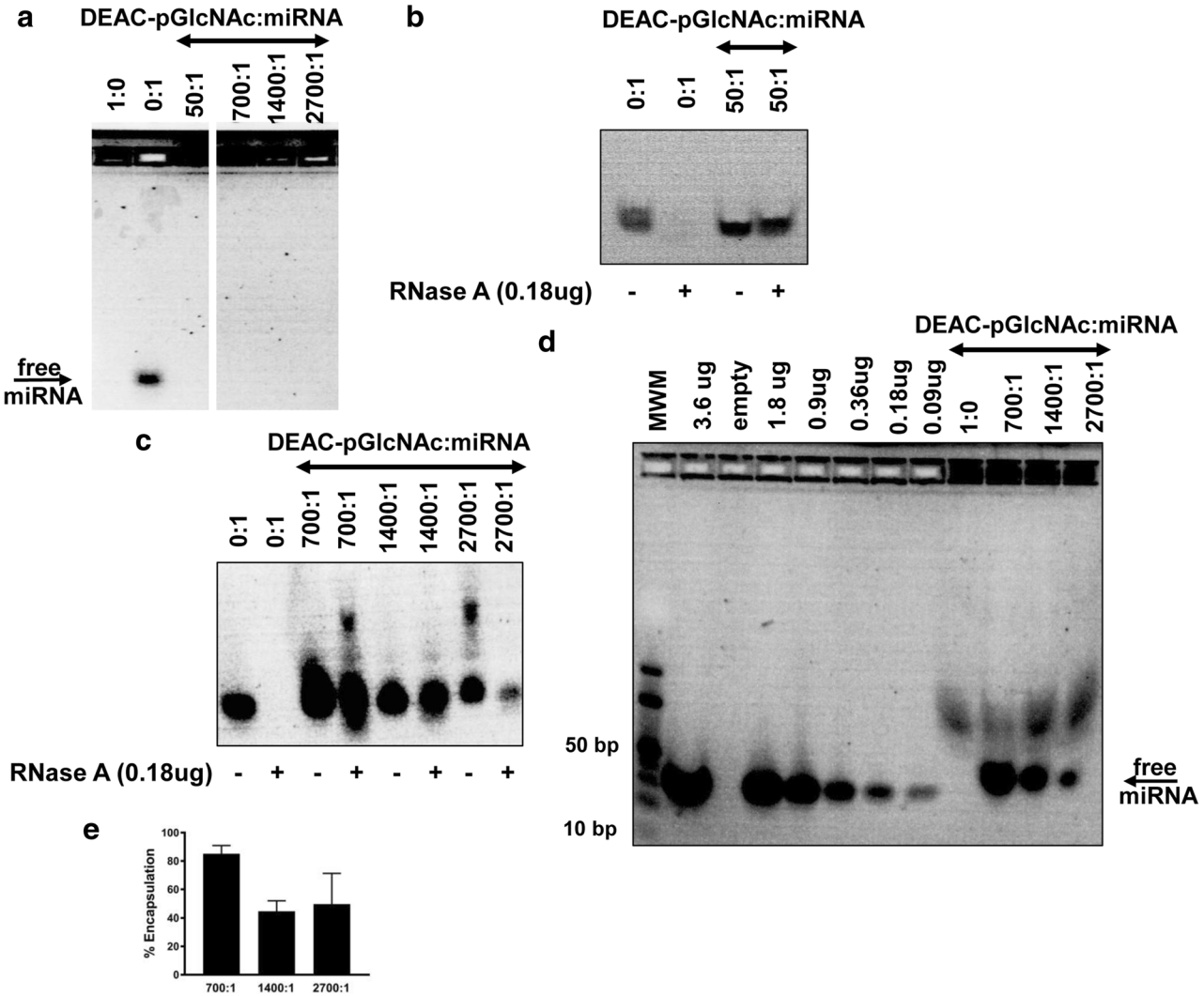

Fig. 1. Synthesis and characterization of DEAC-pGlcNAc nanoparticles. **a** Gel retardation of miRNA-126 by DEAC-pGlcNAc in a 5% agarose gel. Representative of three independent assays. **b**, **c** Naked and DEAC-pGlcNAc-complexed miRNAs at 50:1, 700:1, 1400:1, and 2700:1 ratios were incubated in the presence and absence of RNase A (0.1μg) for 1 h at 37 °C. **d** Naked miRNA at different microgram concentrations was used to establish a standard curve (lanes 2, 4–8) using an encapsulation efficiency assay. Nanocomplexes treated with 4% SDS are displayed in lanes 9–12. **e** Quantification of encapsulation efficiency based on the standard curve established using Image J and GraphPad Prism.

localization of the complex by fluorescent microscopy (Fig. 2a). Cy3-positive cells were observed in the 700:1, 1400:1, and 2700:1 N/P ratio groups while Cy3 fluorescence was absent in cells incubated with Cy3-miRNA-126-5p alone (data not shown).

Cationic polymers can impact the metabolic activity and viability of the cell, thus we wanted to determine the impact of DEAC-pGlcNAc:miR-126 on cellular metabolic activity using an MTT colorimetric assay. HUVECs were exposed to DEAC-pGlcNAc:miR-126-5p nanoparticles for 24 h at N/P ratios of 700:1, 1400:1, and 2700:1. Cells incubated in media without particles were used as a control. Differences in cell metabolic activity were not observed between control and experimental groups (Fig. 2b). Based on these findings, the 700:1 N/P ratio was used for further characterization.

Characterization of the DEAC-pGlcNAc:miRNA Nanocomplex

Dynamic light scattering (DLS) is a measurement of fluctuations in scattered light intensity due to

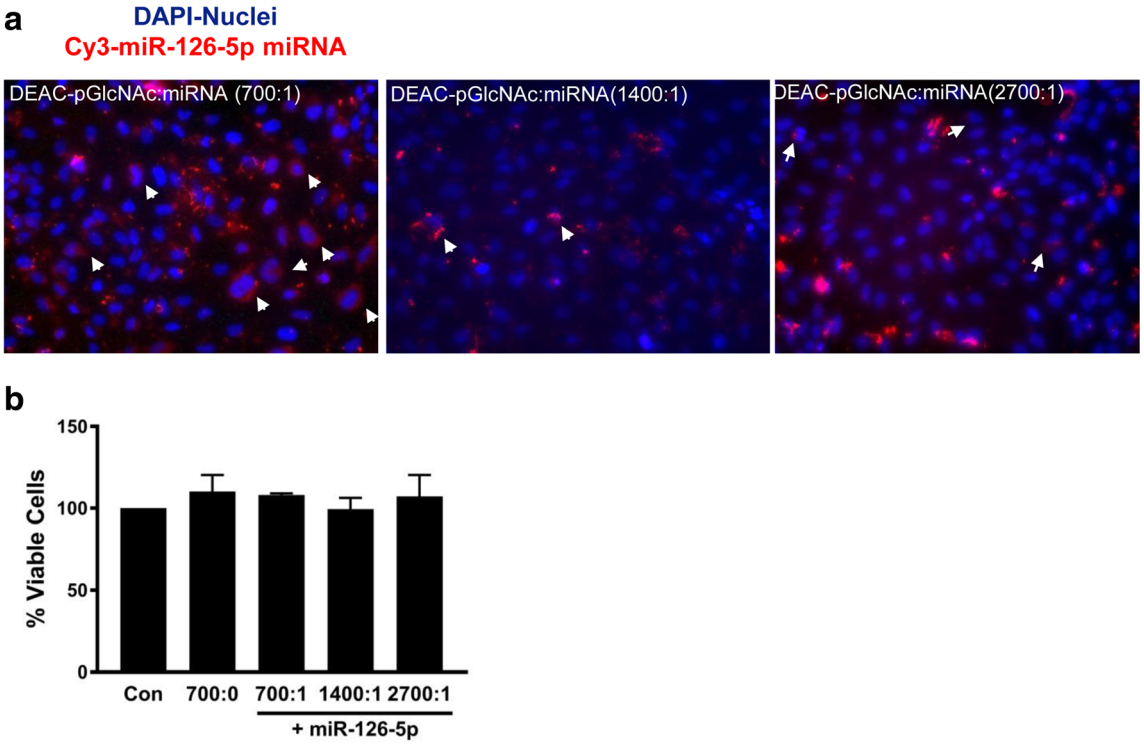

Fig. 2. Optimization of *in vitro* cellular delivery of DEAC-pGlcNAc:miRNAs. **a** Fluorescent microscopy analysis of Cy3-labeled miRNA-126-5p (Cy3-miRNA-126; red) uptake in HUVECs post-24-h incubation at 37 °C. Nuclei were counterstained with DAPI (blue). The arrows point to Cy3 co-localization with DAPI-stained nuclei. **b** HUVECs incubated for 24 h with DEAC-pGlcNAc alone or in complex with varying amounts of miRNA.

Brownian motion of spherically shaped particles. Based on using DLS analysis, we observed that DEAC-pGlcNAc polymers alone had an average size of 287 nm (Fig. 3a). The 700:1 was 204 nm (Fig. 3a). The 700:1 nanoparticles had a zeta potential of +16.4 mV and a polydispersity index (PDI) of 0.479 suggesting that the nanoparticles were fairly monodisperse (Fig. 3b, c). TEM imaging further confirmed that the 700:1 nanoparticles were spherical in shape and monodispersed (Fig. 3d).

The DEAC-pGlcNAc:miRNA Nanocomplex Delivers miR-126 Expression *In Vitro*

To further quantify miRNA delivery following treatment of HUVECs with nanocomplexes, we performed qPCR. Incubation with DEAC-pGlcNAc:miR-126-3p complexes demonstrated significant increases in miR-126-3p expression (nine fold) compared to control and DEAC-pGlcNAc alone (Fig. 4a), while incubation with DEAC-pGlcNAc:miR-126-5p complexes resulted in a non-significant trend toward increased cellular miR-126-5p (Fig. 4b). We further examined miRNA delivery in NIH 3T3 cells which have low basal miR-126-3p and -5p levels. Incubation of NIH 3T3 cells with DEAC-pGlcNAc**:**miR-126-3p nanocomplexes resulted in a 1525 ± 310-fold cellular increase (Fig. 4c). Similarly, incubation with 5p complexes augmented expression 3772 ± 3248-folds which failed to meet statistical significance due to inter-experimental variability (Fig. 4d). Collectively, these data suggest that DEAC-pGlcNAc complexes can efficiently deliver miRNAs to enhance their cellular concentrations *in vitro*.

Previous studies have shown that miR-126-3p suppresses Spred-1 mRNA translation [8]. Spred-1 directly targets Rac-1 with subsequent suppression of ERK phosphorylation. Thus, we examined whether utilizing a 50:1 N/P molar ratio nanoparticles with reduced DEAC-pGlcNAc concentrations would induce *in vitro* biological effects as we previously demonstrated that the 50:1 complex sufficiently binds miRNA (Fig. 1b) and protects against RNase A degradation (Fig. 1c).

a

N/P ratio	Mean Diameter (d.nm)	Polydispersity (PDI)	Zeta Potential (mV)
DEAC-pGlcNAc (700:0)	287.5	0.389	+23.5
700:1	204.6	0.479	+16.4

b

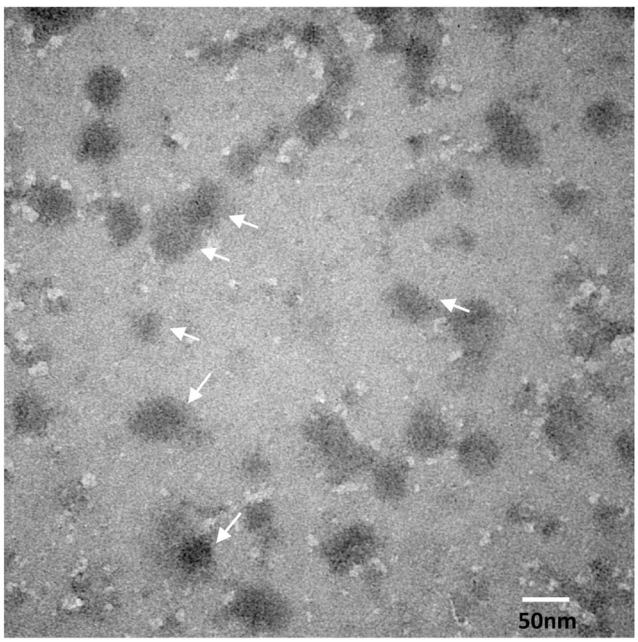

Fig. 3. Analysis of nanoparticles using dynamic light scattering (DLS) and TEM. Size distribution of **a** DEAC-pGlcNAc alone and **b** DEAC-pGlcNAc:miRNA nanoparticles size at a 700:1 M ratio as measured by DLS after resuspension in an acidic (HCl) water solution, pH 3.0. **c** Table showing measurements of average nanoparticle size, polydispersity, and zeta potential. **d** DEAC-pGlcNAc/miRNA nanoparticles visualized using transmission electron microscopy (TEM); scale bar 50 nm at a magnification of × 200,000 and 80 kV power.

In efforts to further characterize the 50:1 N/P ratio particle size and effective delivery of miRNA, TEM, DLS, and qRT-PCR were performed. Using DLS technology, we confirmed that the mean diameter of the complexes was 190 nM with a polydispersity index (PDI) of 0.34 (Fig. 5a). To assess the functionality of the 50:1 complex, first we performed qPCR following HUVEC treatment with the 50:1 complex after 24 h. Quantitation by RT-PCR was used to measure the changes in miR-126 expression compared to control (Fig. 5b, c). In cells pre-incubated with 50:1 DEAC-pGlcNAc:miR-126-3p nanoparticles, FGF significantly increased the phosphorylation of ERK at 15 min in cells compared to DEAC-pGlcNAc:NsiRNA controls ($p < 0.001$) (Fig.5d). Similarly, treatment of HUVECs with 50:1 DEAC-pGlcNAc:miR-126-5p nanocomplexes significantly reduced baseline expression of the miR-126-5p target DLK-1 (Fig. 5e).

DEAC-pGlcNAc:miR-126-5p Nanoparticles Improve Survival in Septic Mice

Although our *in vitro* studies showed that the 50:1 N/P ratio had more robust biological effects, based on the RNase A assay, we postulated that higher concentrations of DEAC-pGlcNAc may provide better protection from circulating RNases *in vivo*. Thus, we utilized the 700:1 complex for *in vivo* studies. Delivery of miR-

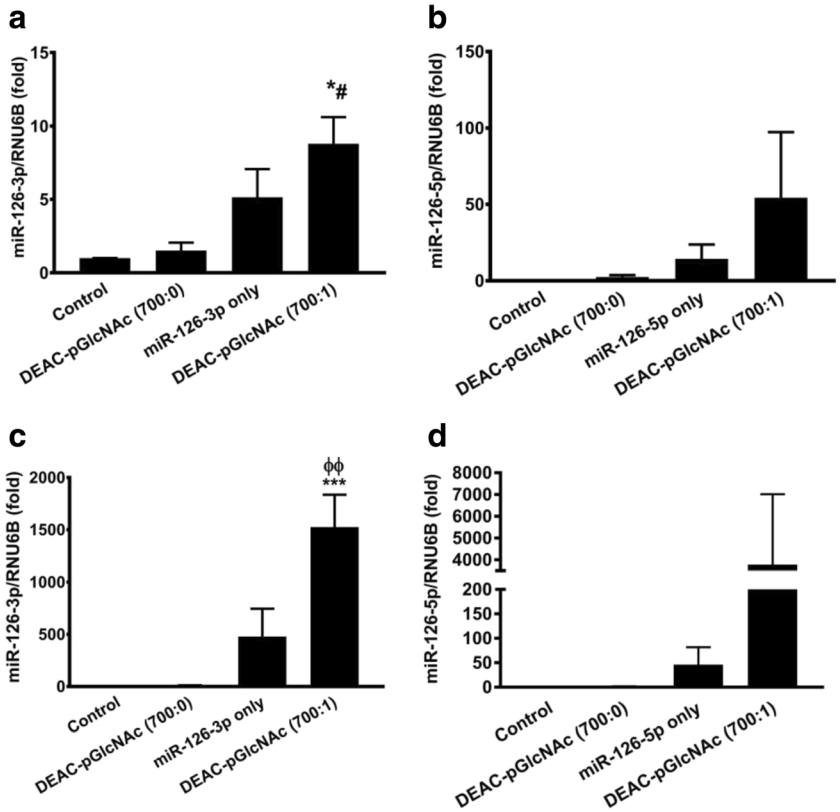

Fig. 4. DEAC-pGlcNAc mediates miRNA-126 delivery real-time PCR analysis of **a** miR-126-3p and **b** -5p levels in HUVECs after 24 h. miR-126 levels were normalized to U6. Real-time PCR analysis of NIH 3T3 fibroblast cell line **c** miR-126-3p and **d** -5p levels after 24 h DEAC-pGlcNAc complex treatment. miR-126 levels were normalized to U6. Data are mean ± SEM of three independent samples performed in duplicate, where $*p < 0.05$, $***p < 0.001$ compared to control, $\#p < 0.05$ compared to DEAC-pGlcNAc, and $\phi\phi p < 0.01$ compared to miR-126 alone using one-way ANOVA.

126 has previously been shown to have therapeutic effects on vascular pathologies [21]; thus, we wanted to determine if DEAC-pGlcNAc:miR-126 delivery would improve survival outcomes in septic mice. Sepsis was induced by CLP in CD-1 male mice followed by antibiotic treatment. PBS, DEAC-pGlcNAc alone, DEAC-pGlcNAc:miR-126-3p, or DEAC-pGlcNAc:miR-126-5p was administered *via* intravenous tail vein injection at 2-h and 6-h post-CLP surgery. Treatment with DEAC-pGlcNAc:miR-126-5p significantly improved survival at 168-h (7 days) post-CLP surgery compared to PBS controls (66.6% *vs* 25%; $p < 0.01$) while treatment with DEAC-pGlcNAc:miR-126-3p did not change survival (6.25% *vs* 25%; $p < 0.01$) (Fig. 6). While we observed improved survival with delivery of DEAC-pGlcNAc alone, this increase in survival was not significantly different ($p = 0.055$) than the survival of CLP-PBS controls.

DEAC-pGlcNAc Nanoparticles Decrease Vascular Leakage and Suppress the Inflammatory Immune Response in CLP-Induced Sepsis

Mice underwent sham or CLP surgery and were injected with DEAC-pGlcNAc nanoparticles at 2-h and 6-h post-CLP. An Evans blue dye assay revealed that DEAC-pGlcNAc, DEAC-pGlcNAc -3p, and DEAC-pGlcNAc-5p nanoparticles significantly decreased lung vascular leakage (48 ± 28%, 42 ± 29%, 40 ± 32%, respectively, $p < 0.01$) and kidney vascular leakage (61 ± 23%, 43 ± 33%, 49 ± 26%, respectively, $p < 0.01$, Fig. 7a). Serum samples were collected 24-h post-CLP. DEAC-pGlcNAc and DEAC-pGlcNAc:miR-126-5p significantly reduced serum IL-6 (12 ± 0.7 and 6.9 ± 0.4, $p < 0.01$) and KC (9.4 ± 0.25 and 4.7 ± 0.10, $p < 0.01$) levels. In contrast, DEAC-pGlcNAc-miR-126-3p had no significant effect on those important inflammatory mediators. DEAC-pGlcNAc, DEAC-

a

N/P ratio	Mean Diameter (d.nm)	Polydispersity (PDI)
50:1	190	0.34

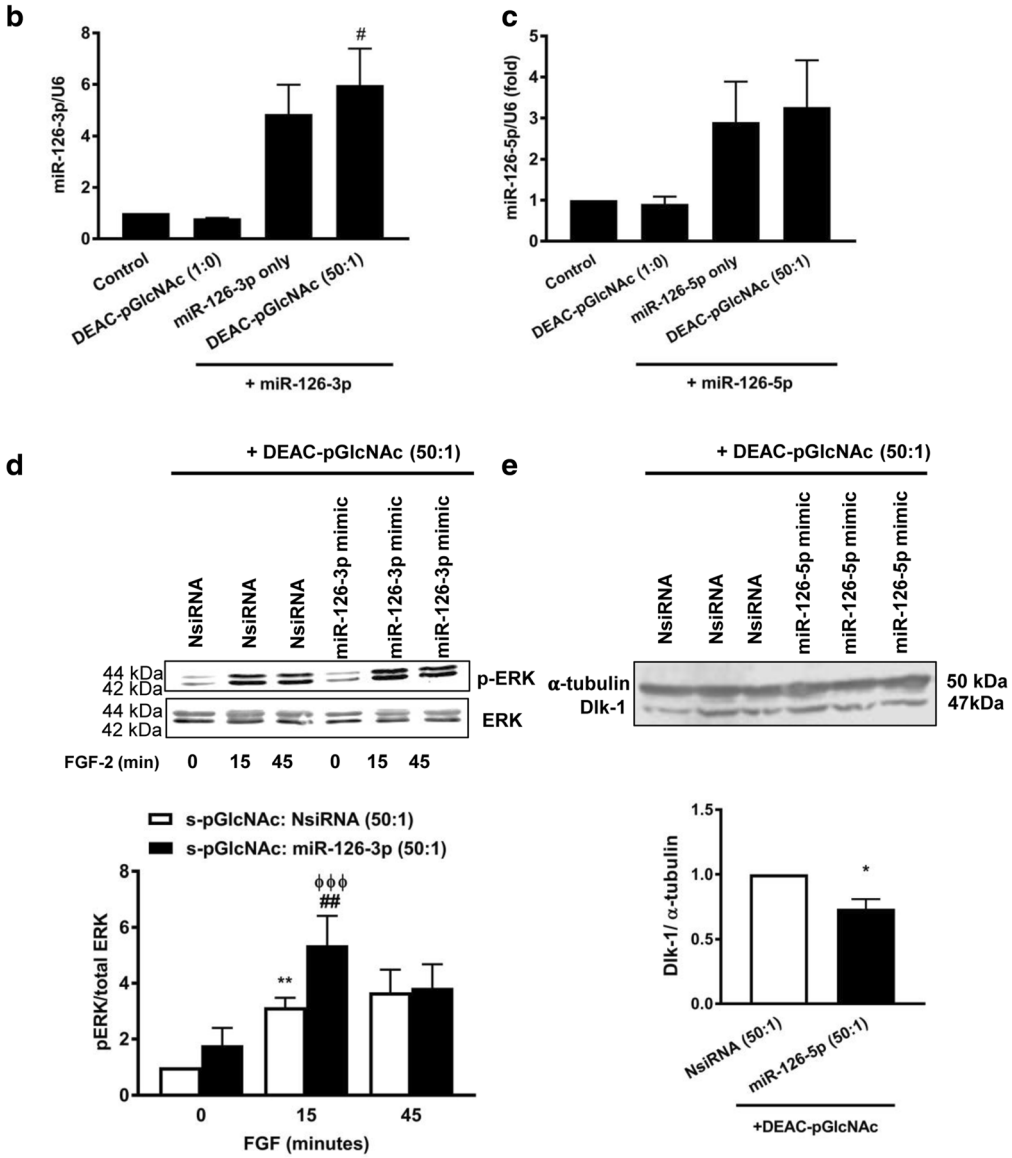

Fig. 5. DEAC-pGlcNAc 50:1 complex mediates enhanced pERK expression and suppression of DLK-1 in HUVECs **a** A table showing average 50:1 nanoparticle size and polydispersity. **b**, **c** Quantitative RT-PCR analysis of the relative expression of miR-126-3p and -5p levels in HUVECs treated with 50:1 DEAC-pGlcNAc:miR-126-3p or -5p nanocomplexes for 24 h. Samples were normalized to U6. #$p < 0.05$ compared to DEAC-pGlcNAc as assessed by one-way ANOVA. **d** Western blot and densitometry bar graph of pERK and ERK expression induced by FGF (10 ng/ml) at 0 min, 15 min, and 45 min following DEAC-pGlcNAc:nsiRNA or -miR-126-3p nanopolymer treatment (50:1) for 30 h. **e** Western blot and densitometry bar graph of DLK-1 expression levels in HUVECs following a 48-h incubation with DEAC-pGlcNAc:NsiRNA or -miR-126-5p nanopolymer treatment (50:1). Analysis for panels D & E was performed using a two-way ANOVA with matching. Data are mean ± SEM of six independent experiments, where *$p < 0.05$, **$p < 0.01$ compared to NsiRNA control, ##$p < 0.01$ compared to the DEAC-pGlcNAc:miR-126-3p control, and ϕϕϕ $p < 0.001$ compared to DEAC-pGlcNAc:miR-126-3p + 15 min FGF (10 ng/ml).

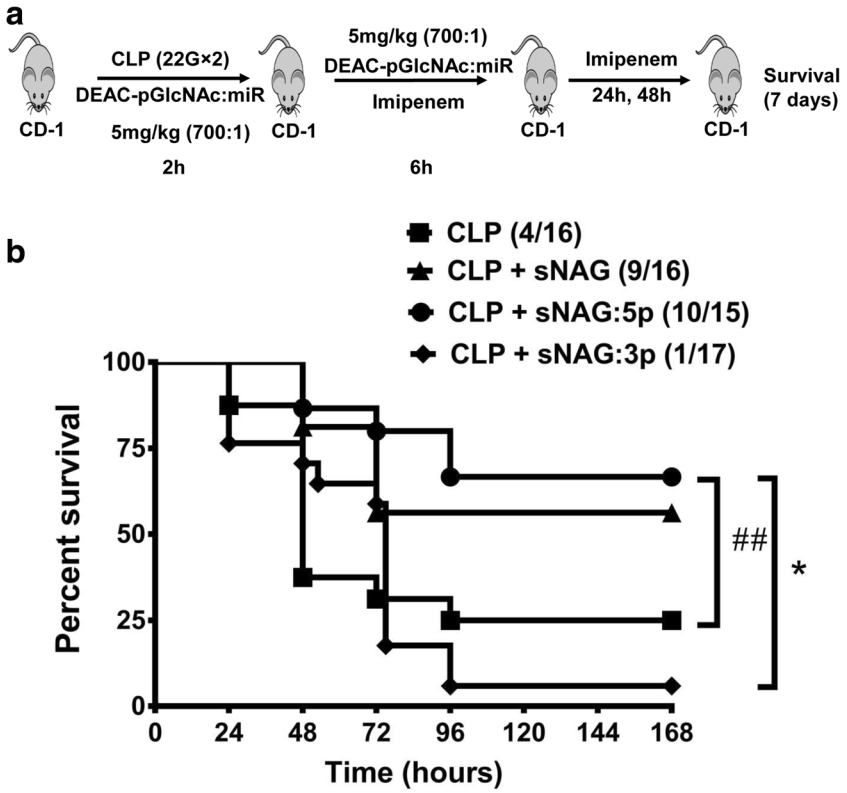

Fig. 6. Delivery of miR-126-5p improves survival in CLP mice. **a** CD-1 mice (15–16 per group) were subjected to CLP surgery. Mice received tail vein injections of either PBS ($n = 16$), DEAC-pGlcNAc ($n = 16$), and DEAC-pGlcNAc:miR-126-3p ($n = 16$) or -5p ($n = 15$) nanopolymer treatments at 2-h and 6-h post-CLP surgery. Mice received intermittent treatments of imipenem at 6-h, 24-h, and 48-h post-CLP. **b** Survival of CLP mice exposed to PBS, DEAC-pGlcNAc, DEAC-pGlcNAc:miR-126-3p, and DEAC-pGlcNAc:miR-126-5p with survival monitored for 7 days. Differences in survival were assessed using the Gehab-Breslow-Wilcoxon test, where $^{**}p < 0.01$ compared to CLP-PBS and $\#p < 0.05$ compared to CLP + DEAC-pGlcNAc:3p.

pGlcNAc:miR-126-5p, and DEAC-pGlcNAc:miR-126-3p significantly reduced IL-1β, MP-1α, MCP-1, and IL-10 (Fig. 7b).

DISCUSSION

The development of miRNA therapies requires effective platforms for miRNA delivery into the cytoplasm of cells. Current delivery systems including viral vectors, liposomes, and chitosan have proven to be suboptimal due to their complex assembly and inefficient delivery of nucleic acids *in vitro* and *in vivo* [22]. To reduce these limitations, we used a DEAC-pGlcNAc nanoparticle/miRNA complex that, when formed, yielded efficient delivery of miRNAs to HUVECs and NIH 3T3 fibroblasts. Our results demonstrate that the DEAC-pGlcNAc:miRNA-126-5p nanocomplex enhances intracellular levels of miR-126 *in vitro* and improves sepsis outcomes *in vivo*.

There are several potential advantages of the DEAC-pGlcNAc polymer as a miRNA delivery platform in sepsis. Its known antimicrobial effects make it an ideal delivery platform for sepsis [18]. Linder et al. previously demonstrated that poly-N-acetyl glucosamine (sNAG) nanofibers, an analog of DEAC-pGlcNAc, have antibacterial effects in wound healing. Specifically, they showed that sNAG enhanced both α- and β-defensin expression in endothelial cells and keratinocytes while reducing bacterial infections in cutaneous wounds infected with *Staphylococcus aureus* [18]. Thus, its antibacterial effects are a potential advantage to its use as a miRNA delivery vehicle in sepsis. Its ability to efficiently encapsulate miRNA and protect it from RNase degradation is critically important to ensuring stability of miRNA in the *in vivo* environment. Further, the nanocomplex diameter (~200 nm) allows it to avoid uptake by the liver and reticuloendothelial system during

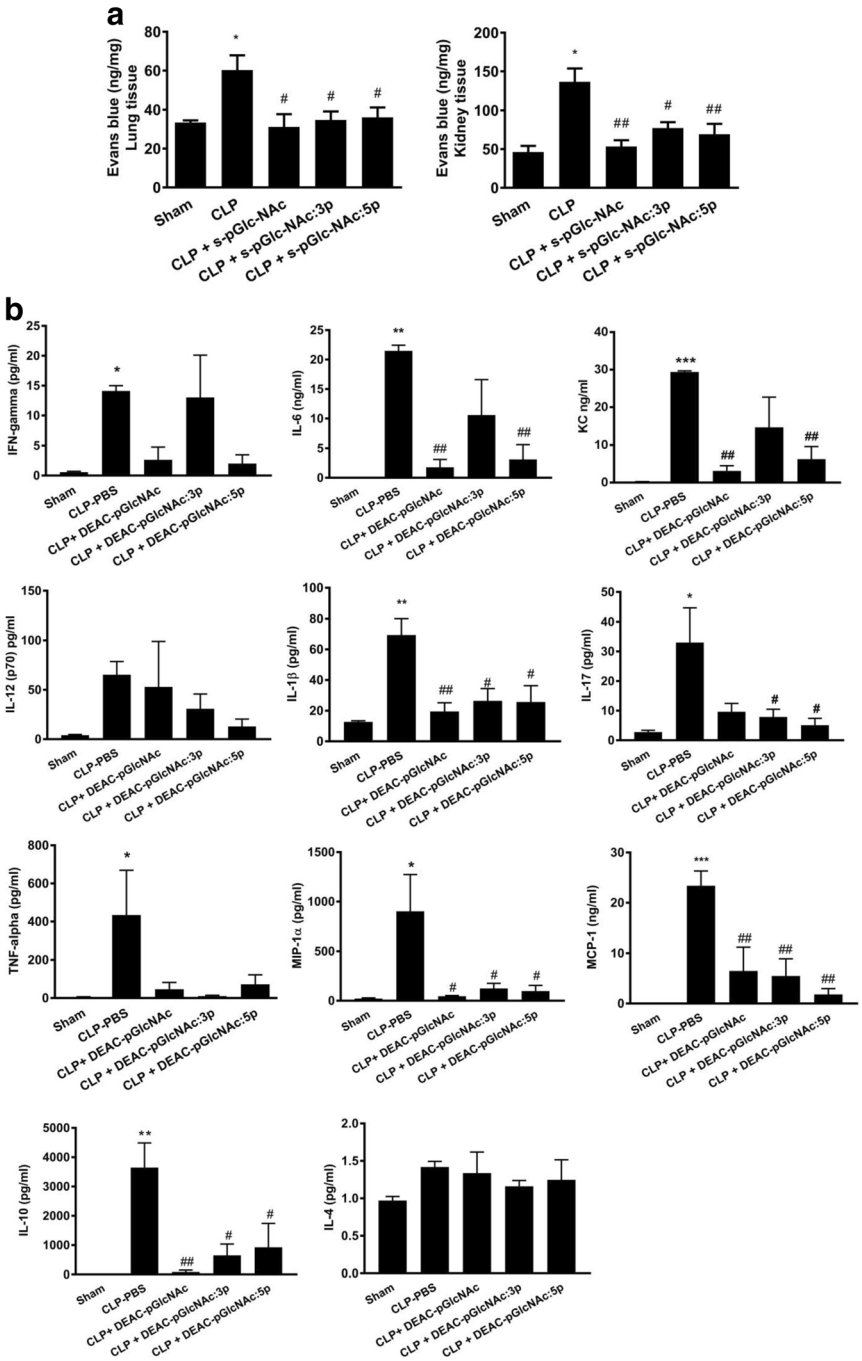

Fig. 7. DEAC-pGlcNAc nanoparticle effects on vascular leakage and inflammatory mediators in CLP-induced sepsis. CD-1 male mice were subjected to CLP surgery. Animals received tail vein injections of either PBS, DEAC-pGlcNAc, DEAC-pGlcNAc:miR-126-3p, or -5p nanopolymer treatments at 2-h and 6-h post-CLP surgery. **a** Vascular leakage in the lung and kidney were determined using an Evans blue dye assay 24-h post-CLP surgery. **b** Serum was collected from whole blood and analyzed for cytokines. Data were analyzed using a one-way ANOVA or the Kruskal-Wallis test, $n = 4–7$ mice per group, $*p < 0.05$, $**p < 0.01$, $***p < 0.001$ compared to sham, $\#p < 0.05$, and $\#\#p < 0.01$ compared to CLP-PBS.

circulation while its cationic zeta potential suggests moderate stability [23].

Our data demonstrate that DEAC-pGlcNAc:miRNA complexes effectively deliver miRNA to cells leading to

alterations in cellular function. It is worth noting that the magnitude of delivered intracellular miRNA appeared to differ by cell type with HUVECs exhibiting significantly smaller increases in miR-126 levels than 3T3 fibroblasts. Although this could be a property of cell-specific delivery efficiency, we suspect that this observation is more likely dictated by the significantly higher baseline levels of miR-126 [12] in endothelial cells as compared to fibroblasts where miR-126 is not normally expressed. This is supported by the robust amount of intracellular fluorescently tagged miR-126 seen within HUVECs after treatment with the nanocomplexes. Interestingly, although the 700:1 concentration of nanocomplexes appeared to provide optimal miRNA protection, our *in vitro* data suggested that this concentration did not allow for optimal miRNA activity upon intracellular delivery (data not shown). We hypothesized that this concentration may impede miRNA release from the nanocomplex leading to impaired miRNA function. Notably, the 50:1 concentration of DEAC-pGlcNAc:miRNA still delivered intact miRNA intracellularly while allowing the miRNA to dissociate from the complex and inhibit gene translation. Future investigation into the optimal concentration for both miRNA delivery and function will be important.

Our findings revealed that DEAC-pGlcNAc nanoparticles loaded with miR-126-5p significantly improved survival in animals subjected to CLP compared to PBS controls. These findings complement our previous studies showing that EPCs that are rich in miR-126-5p significantly improve CLP survival [12]. Survival rates between 5p and 3p nanoparticles were statistically different with 3p also failing to improve survival compared to PBS treatment in sepsis. This suggests that the delivery of miR-126-3p using DEAC-pGlcNAc nanoparticles was ineffective and potentially deleterious. Interestingly, there appeared to be a trend toward improved survival when treating with DEAC-pGlcNAc nanoparticles alone (not coupled to miR-126-3p or -5p) compared to the PBS control. However, there was no significant difference compared to miR-126-5p-loaded nanoparticles.

Circulating cytokines and oxidative stress leads to endothelial dysfunction and increased vascular permeability in CLP sepsis. We observed that all formulations of nanoparticles with or without miRNA preserved vascular integrity compared to CLP-PBS animals 24-h post-CLP surgery. However, vascular integrity measured at 24 h may not be predictive of long-term outcome in CLP sepsis. Interestingly, DEAC-pGlcNAc and DEAC-pGlcNAc:miR-126-5p but not DEAC-pGlcNAc:miR-126-3p treatment reduced the hallmark sepsis cytokine levels of IL-6, KC, and IFN-gamma. The aforementioned cytokines are most predictive of sepsis outcomes. The failure to decrease these inflammatory mediators may provide a partial explanation for why DEAC-pGlcNAc:miR-126-3p failed to improve the mortality.

One possible explanation for the ineffectiveness of miR-126-3p might be that it functions as a miR-126-5p antagomir thus reducing the effects of innate miR-126-5p. In human sepsis [13], there is an increase in plasma miR-126 levels and if similar trends persist in experimental animal models of sepsis, excess miR-126-3p may neutralize the beneficial effects of miR-126-5p. Further, the miR-126/VEGF axis modulates angiogenesis and junctional protein stability *in vivo* which have been linked to increased vascular permeability in sepsis. MiR-126-3p promotes activation of VEGF-mediated pathways including the phosphorylation of ERK, which has been proven to be detrimental to vascular integrity in pathophysiologic conditions [24, 25].

One limitation of this study was that we dosed mice based on the polymer concentration (5 mg/kg) rather than the miRNA concentration. Thus, we only administered 720 ng (18 ng/g) of miRNA to CLP mice. The large amounts of DEAC-pGlcNAc delivered may have blunted the potential impacts of 5p on the disease process. In addition, we only treated animals at 2-h and 6-h post-surgery as opposed to continuous treatments over the course of sepsis. Future studies will examine the impacts of 50:1 nanocomplexes that contain increased amounts of miRNA in order to determine the presence of a dose-response effect. Additionally, targeting of nanocomplexes to the endothelium using the $\alpha v\beta 3$ integrin ligand LXW7 modification [26] or RGD peptide might allow us to target the endothelium *in vivo* and parse out the effects of miR-126-5p on endothelial function in the sepsis microenvironment.

CONCLUSION

The DEAC-pGlcNAc polymer serves as a viable option for delivery of miRNAs; DEAC-pGlcNAc:miR-126-5p nanoparticle complexes improved survival in CLP animals and reduced the inflammatory cytokine response. Collectively, these studies raise the possibility that DEAC-pGlcNAc and/or complexed with miR-126-5p may represent a novel therapeutic approach for human sepsis.

ACKNOWLEDGEMENTS

We thank Ametria Harrison and Pengfei Li for their technical support throughout this project. Additionally, we

thank Robin Muise-Helmericks and Amanda LaRue for their experimental expertise and project support.

Funding This work was supported by the NIGMS 1R01GM113995 (HF). This work was also supported by grants NHLBI 5T32HL007260–39 (JJB), 1K23HL135263-01A1 (AG), and UL1 TR 001450 (PVH), and financial and technical supports were provided in part by Marine Polymer Sciences, Inc. Burlington, MA (JV and MD).

COMPLIANCE WITH ETHICAL STANDARDS

Conflict of Interest. The authors declare that they have no conflict of interest.

Ethics Approval. Animal studies were conducted in accordance with the Guide for the Care and Use of Laboratory Animals published by the National Institutes of Health and were approved by the Institutional Animal Care and Use Committee at the Medical University of South Carolina.

REFERENCES

1. Torio CM, Andrews RM. National inpatient hospital costs: the most expensive conditions by payer, 2011: Statistical Brief #160. Healthcare Cost and Utilization Project (HCUP) Statistical Briefs. Rockville (MD), 2006.
2. Murphy, S.L., J. Xu, and K.D. Kochanek. 2013. Deaths: final data for 2010. *National Vital Statistics Reports* 61: 1–117.
3. Torio CM, Moore BJ. National inpatient hospital costs: the most expensive conditions by payer, 2013: Statistical Brief #204. Healthcare Cost and Utilization Project (HCUP) Statistical Briefs. Rockville (MD), 2006.
4. Angus, D.C., and T. van der Poll. 2013. Severe sepsis and septic shock. *The New England Journal of Medicine* 369: 2063.
5. Pratt, A.J., and I.J. MacRae. 2009. The RNA-induced silencing complex: a versatile gene-silencing machine. *The Journal of Biological Chemistry* 284: 17897–17901.
6. Neth, P., M. Nazari-Jahantigh, A. Schober, and C. Weber. 2013. MicroRNAs in flow-dependent vascular remodelling. *Cardiovascular Research* 99: 294–303.
7. Chistiakov, D.A., A.N. Orekhov, and Y.V. Bobryshev. 2016. The role of miR-126 in embryonic angiogenesis, adult vascular homeostasis, and vascular repair and its alterations in atherosclerotic disease. *Journal of Molecular and Cellular Cardiology* 97: 47–55.
8. Wang, S., A.B. Aurora, B.A. Johnson, X. Qi, J. McAnally, J.A. Hill, J.A. Richardson, R. Bassel-Duby, and E.N. Olson. 2008. The endothelial-specific microRNA miR-126 governs vascular integrity and angiogenesis. *Developmental Cell* 15: 261–271.
9. Fish, J.E., M.M. Santoro, S.U. Morton, S. Yu, R.F. Yeh, J.D. Wythe, K.N. Ivey, B.G. Bruneau, D.Y.R. Stainier, and D. Srivastava. 2008. miR-126 regulates angiogenic signaling and vascular integrity. *Developmental Cell* 15: 272–284.
10. Kuhnert, F., M.R. Mancuso, J. Hampton, K. Stankunas, T. Asano, C.Z. Chen, and C.J. Kuo. 2008. Attribution of vascular phenotypes of the murine Egfl7 locus to the microRNA miR-126. *Development* 135: 3989–3993.
11. Tang, R., L. Pei, T. Bai, and J. Wang. 2016. Down-regulation of microRNA-126-5p contributes to overexpression of VEGFA in lipopolysaccharide-induced acute lung injury. *Biotechnology Letters* 38: 1277–1284.
12. Fan, H., A.J. Goodwin, E. Chang, B. Zingarelli, K. Borg, S. Guan, P.V. Halushka, and J.A. Cook. 2014. Endothelial progenitor cells and a stromal cell-derived factor-1alpha analogue synergistically improve survival in sepsis. *American Journal of Respiratory and Critical Care Medicine* 189: 1509–1519.
13. Goodwin, A.J., C. Guo, J.A. Cook, B. Wolf, P.V. Halushka, and H. Fan. 2015. Plasma levels of microRNA are altered with the development of shock in human sepsis: an observational study. *Critical Care* 19: 440.
14. Zhou, Y., P. Li, A.J. Goodwin, J.A. Cook, P.V. Halushka, E. Chang, and H. Fan. 2018. Exosomes from endothelial progenitor cells improve the outcome of a murine model of sepsis. *Molecular Therapy* 26: 1375–1384.
15. Schober, A., M. Nazari-Jahantigh, Y. Wei, K. Bidzhekov, F. Gremse, J. Grommes, R.T.A. Megens, K. Heyll, H. Noels, M. Hristov, S. Wang, F. Kiessling, E.N. Olson, and C. Weber. 2014. MicroRNA-126-5p promotes endothelial proliferation and limits atherosclerosis by suppressing Dlk1. *Nature Medicine* 20: 368–376.
16. Juliano, R.L., R. Alam, V. Dixit, and H.M. Kang. 2009. Cell-targeting and cell-penetrating peptides for delivery of therapeutic and imaging agents. Wiley Interdisciplinary Reviews. *Nanomedicine and Nanobiotechnology* 1: 324–335.
17. Vournakis JN, Finkielsztein S, Pariser ER, Helton M. Bicompatible poly-β-1→4-N-acetylglucosamine. **Google Patents**, 2004.
18. Lindner, H.B., A. Zhang, J. Eldridge, M. Demcheva, P. Tsichlis, A. Seth, et al. 2011. Anti-bacterial effects of poly-N-acetylglucosamine nanofibers in cutaneous wound healing: requirement for Akt1. *PLoS One* 6: e18996.
19. Lindner, H.B., L.M. Felmly, M. Demcheva, A. Seth, R. Norris, A.D. Bradshaw, et al. 2015. pGlcNAc nanofiber treatment of cutaneous wounds stimulate increased tensile strength and reduced scarring via activation of Akt1. *PLoS One* 10: e0127876.
20. Kong, X.Y., Y.Q. Du, L. Li, J.Q. Liu, G.K. Wang, J.Q. Zhu, et al. 2010. Plasma miR-216a as a potential marker of pancreatic injury in a rat model of acute pancreatitis. *World Journal of Gastroenterology : WJG* 16: 4599–4604.
21. Zhou, F., X. Jia, Y. Yang, Q. Yang, C. Gao, S. Hu, Y. Zhao, Y. Fan, and X. Yuan. 2016. Nanofiber-mediated microRNA-126 delivery to vascular endothelial cells for blood vessel regeneration. *Acta Biomaterialia* 43: 303–313.
22. Eliyahu, H., Y. Barenholz, and A.J. Domb. 2005. Polymers for DNA delivery. *Molecules* 10: 34–64.
23. Bamrungsap, S., Z. Zhao, T. Chen, L. Wang, C. Li, T. Fu, and W. Tan. 2012. Nanotechnology in therapeutics: a focus on nanoparticles as a drug delivery system. *Nanomedicine (London, England)* 7: 1253–1271.
24. Narasimhan, P., J. Liu, Y.S. Song, J.L. Massengale, and P.H. Chan. 2009. VEGF stimulates the ERK 1/2 signaling pathway and apoptosis in cerebral endothelial cells after ischemic conditions. *Stroke* 40: 1467–1473.

25. Gavard, J., and J.S. Gutkind. 2006. VEGF controls endothelial-cell permeability by promoting the beta-arrestin-dependent endocytosis of VE-cadherin. *Nature Cell Biology* 8: 1223–1234.
26. Hao, D., W. Xiao, R. Liu, P. Kumar, Y. Li, P. Zhou, F. Guo, D.L. Farmer, K.S. Lam, F. Wang, and A. Wang. 2017. Discovery and characterization of a potent and specific peptide ligand targeting endothelial progenitor cells and endothelial cells for tissue regeneration. *ACS Chemical Biology* 12: 1075–1086.